ELSEVIER

Catalysis Today 69 (2001) 147–152

CATALYSIS TODAY

www.elsevier.com/locate/cattod

Influence of operating conditions on the observed reaction rate in the single channel monolith reactor

Gorazd Berčič*

Laboratory for Catalysis and Chemical Reaction Engineering, National Institute of Chemistry, Hajdrihova 19, 1001 Ljubljana, Slovenia

Abstract

The catalytic hydrogenation of nitrobenzoic acid (NBA) to the aminobenzoic acid was used as a model reaction for a quantitative study of influences of the operating conditions on the observed reaction rate in a single channel monolith reactor operated in Taylor flow regime. A simple mathematical model was derived and used for the analysis of hydrogenation experiments carried out in batch mode. Results showed that in the investigated concentration range of NBA, i.e. 0.0005–0.02 mol/l and under the hydrogen pressure of 1 bar, the observed reaction rate is considerably limited by mass transport. At higher concentrations of NBA, the reaction is controlled by the hydrogen mass transport while at lower concentrations the mass transport of NBA is dominant. The analysis of experimental results, which were obtained when the length of gas bubbles and liquid slugs were varied, showed that the reaction took place in the thin liquid film surrounding the gas bubble. The liquid slug serves as exchanger of reactants and reaction products between bulk liquid slug and liquid film surrounding the catalyst surface. © 2001 Elsevier Science B.V. All rights reserved.

Keywords: Monolith catalyst; Taylor flow; Nitrobenzoic acid; Hydrogenation; Train flow; Segmented flow; Three-phase reactor; Film model

1. Introduction

The monolith blocks, usually coated or impregnated with catalytic active substances, are already widely used as a heterogeneous catalyst for reactions among substances from a gaseous phase, especially to prevent the harmful gasses being discharged into the atmosphere [1]. While in such devices homogeneous flow distribution in channels of the monolith block is easily achieved, this is not the case when monoliths are used for purposes of two-phase reactions. Some studies have already been made in such conditions [1–6]. Those studies clearly demonstrate the potentials of monolith reactors in the area of the two-phase reactors and confirm the well-known advantages (i.e. low pressure drop, high mass transport coefficients, high catalyst efficiency) of monolith reactors compared to the fixed bed three-phase reactors. However, the large-scale commercial installations of monolith reactors are very rare [1]. The main problems during the scale-up of reactors using catalytic active monolith blocks are liquid distribution problem, internal redistribution and recirculation of gas phase when more large blocks are stacked as well as the lack of verified mathematical models. On the basis of theoretical studies [7,8] and experimental observations [2,6], researchers agree that optimal operation conditions of monolith reactor are determined by intrinsic reaction kinetics and by length and sequence of gas bubbles and liquid slugs. Despite the great potentials of monolith reactors in the area of three-phase reactors, only few studies have been made on the "microscopic" level of one capillary. While

---

* Tel.: +386-61-1760282; fax: +386-61-1259244.
E-mail address: gorazd.bercic@ki.si (G. Berčič).

0920-5861/01/$ – see front matter © 2001 Elsevier Science B.V. All rights reserved.
PII: S0920-5861(01)00390-X

Irandoust et al. [9] and Hatziantoniou and Andersson [10] derived generalized correlations for prediction of mass transport coefficients which combine separate contribution of surfaces exposed to gas bubbles and liquid slugs on the predicted mass transport, we [11] determined correlations on the basis of macroscopic observations and parameters characteristic for Taylor flow.

The main subject of this study was to verify the proposed correlations by a simple reactor model based on the unit cell concept. The proposed model was used to predict the reaction limits for the hydrogenation of NBA in a single channel monolith reactor.

2. Experimental

The experiments were performed in an experimental set-up which is described in detail in [11]. Preparation and properties of the catalyst used in this investigation could be found in [12]. The hydrogenation of nitrobenzoic acid (NBA) was carried out with pure hydrogen on a palladium catalyst. The experiments were performed in the temperature range from 303 to 323 K. The up-flow mode was used. The inlet pressure varied from 1.06 to 1.09 bar. The 96 cm long catalyst tube was placed between two glass tubes of almost the same ID in order to enable the visual observation of the flow pattern. The joint tube was put in a thermostated jacket. The inlet temperature was adjusted by a separate pre-heater which was located next to the tee element. The volume/mass of solution in the CSTR tank was adjusted by weighting the tank. Prior to the experiments the tank was filled with an extra amount of solution in order to let the catalyst come into the steady state. When the balance showed the desired mass, the outlet from the reactor was switched to the recycle loop and the reaction time was set to 0. Analyses were made by measuring the UV–Vis spectra of mixture by spectrophotometer (Perkin Elmer, model Lambda 40). The concentration of NBA and ABA were determined by deconvolution of the measured spectra in the range from 205 to 300 nm using a linear combination of spectrums measured for the pure components. The accuracy of the method was verified by means of calibration mixtures and was below 1 ± 0.01.

3. Mathematical characterization of the reactor model

Results of the previous studies showed that the characteristic element of the segmented two-phase flow (Taylor flow) through the capillary is the length of the unit cell (UCL) which presents the length of one gas bubble and one liquid slug. For one unit cell (UC) of volume V, the general mass balance for component i from the liquid phase is written as

$$\frac{\mathrm{d}C_i}{\mathrm{d}t} V(1-\varepsilon_\mathrm{G}) = k_{\mathrm{L},i} A_\mathrm{L}(C_i^\mathrm{sat} - C_i) - k_{\mathrm{S},i} A_\mathrm{S}(C_i - C_{\mathrm{S},i}). \tag{1}$$

The surface concentration $C_{\mathrm{S},i}$ is implicitly determined by the catalyst activity and mass flux to the catalyst surface. To express the mass transfer coefficients from the former equation in terms of $k_\mathrm{L}a$, and $k_\mathrm{S}a$ coefficients, both sides of equation were divided by $V(1-\varepsilon_\mathrm{G})$. To calculate $k_\mathrm{L}a$ and $k_\mathrm{S}a$ coefficients, the equation proposed by Berčič and Pintar [11] and the modified equation for calculation of $k_\mathrm{S}a$ as proposed by Alibegić [13] were used:

$$k_\mathrm{L}a = \frac{0.111 v^{1.19}}{((1-\varepsilon_\mathrm{G})\mathrm{UCL})^{0.57}},$$

$$k_\mathrm{S}a = \frac{0.059 v^{0.63}}{((1-\varepsilon_\mathrm{G})\mathrm{UCL} - 9.4\mathrm{UCL}\varepsilon_\mathrm{G}(\delta/d_T))^{0.41}}. \tag{2}$$

In Eq. (2), the relative film thickness δ/d_T was calculated using the equation proposed by Irandoust and Andersson [14]. Since the equations for calculation of $k_\mathrm{L}a$ and $k_\mathrm{S}a$ were derived for the case of methane and benzoic acid, the values of coefficients $k_\mathrm{L}a$ and $k_\mathrm{S}a$ for the case of hydrogen, NBA and ABA were estimated on the analogy with mass transfer in stagnant film ($k_\mathrm{L}a$) and mass transfer in laminar flow ($k_\mathrm{S}a$) [15]. The value of $k_\mathrm{S}a$ and $k_\mathrm{L}a$ coefficients for each component were corrected using the following relations:

$$(k_\mathrm{S}a)_i = (k_\mathrm{S}a)_\mathrm{BA}\left(\frac{D_i}{D_\mathrm{BA}}\right)^{0.66},$$

$$(k_\mathrm{L}a)_{\mathrm{H}_2} = (k_\mathrm{L}a)_{\mathrm{CH}_4}\left(\frac{D_{\mathrm{H}_2}}{D_{\mathrm{CH}_4}}\right)^{0.5}. \tag{3}$$

Since the diluted solutions of reactants were used only the diffusion coefficient was considered as compound dependant. Other physical properties and hydrogen solubility were calculated from the correlations for pure water [16–19]. After rearrangement, the UC model was written in terms of $k_\mathrm{L}a$ and $k_\mathrm{S}a$ as follows:

$$\frac{\mathrm{d}C_i}{\mathrm{d}t} = (k_\mathrm{L}a)_i(C_i^\mathrm{sat} - C_i) - (k_\mathrm{S}a)_i(C_i - C_{\mathrm{S},i}). \quad (4)$$

For the CSTR tank, the mass balance for the main reactant, NBA, is written as

$$-\frac{\mathrm{d}C_\mathrm{NBA}}{\mathrm{d}t}V_\mathrm{CSTR} = \Phi_\mathrm{liq}(C_\mathrm{NBA} - C_\mathrm{NBA}^\mathrm{inlet}). \quad (5)$$

The inlet concentration in the CSTR tank $C_\mathrm{NBA}^\mathrm{inlet}$ was equal to the outlet concentration of the NBA from the single channel monolith reactor, which is described by Eq. (4). Eq. (5) was solved for the following initial conditions:

$$\text{At } t = 0: \quad C_\mathrm{NBA} = C_{\mathrm{NBA},0}, \quad C_\mathrm{ABA} = 0, \quad C_{\mathrm{H}_2} = C_{\mathrm{H}_2}^\mathrm{sat}. \quad (6)$$

During the integration of Eq. (5), the inlet concentration of NBA was calculated by solving mass balance equation (4). Eq. (4) was integrated over the residence time τ_cat, which was determined from the catalytic tube volume and total flow rate, i.e. liquid plus gas. The average velocity in the capillary was 8.0 cm/s with the exception of the run 7 (10.7 cm/s). By peristaltic pump the liquid solution was recycled by pumping reaction solution from CSTR tank to the mixing tee. Since the liquid flow was not high compared to the volume of the tube for connection, the residence time of solution in the connection tube was not neglected. From the volume of that tube (4.1 ml) and liquid flow rate, the residence time τ_FS in the feeding system was determined. The impact of this delay during solution of Eq. (4) was considered by the initial conditions as follows:

$$C_\mathrm{inlet} = \begin{cases} C_{\mathrm{NBA},0}(t=0) & \text{for } t \le \tau_\mathrm{FS}, \\ C_\mathrm{NBA}(t-\tau_\mathrm{FS}) & \text{for } t > \tau_\mathrm{FS}. \end{cases} \quad (7)$$

During sampling, the amount of solution in the CSTR tank was reduced for the amount of samples taken out for analysis. This volume reduction was accounted for at sampling times. The system of differential equations was solved using 5th order Cash-Kerp Runge–Kutta integration algorithm [20]. Eq. (5) was integrated in time from one to another sampling point, while equations describing reaction in the monolith reactor were integrated simultaneously within the integration loop from time $t = t - \tau_\mathrm{FS}$ to $t = t$.

4. Experimental results and discussion

In Figs. 1–4, experimental results are shown together with the model predictions. The model was solved for the limiting conditions, i.e. conditions

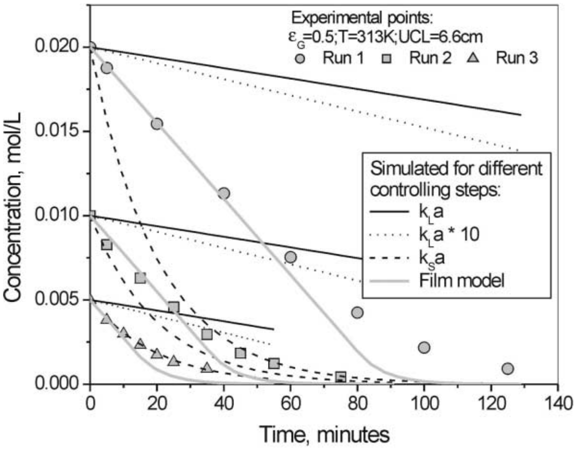

Fig. 1. Measured and simulated concentration profiles during hydrogenation of NBA at 313 K and at gas hold-up of 0.5.

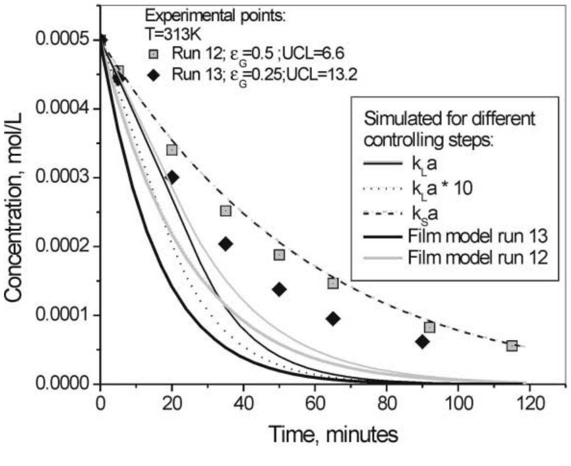

Fig. 2. Comparison between the measured and simulated concentration profiles during hydrogenation of NBA at 313 K and various gas hold-ups.

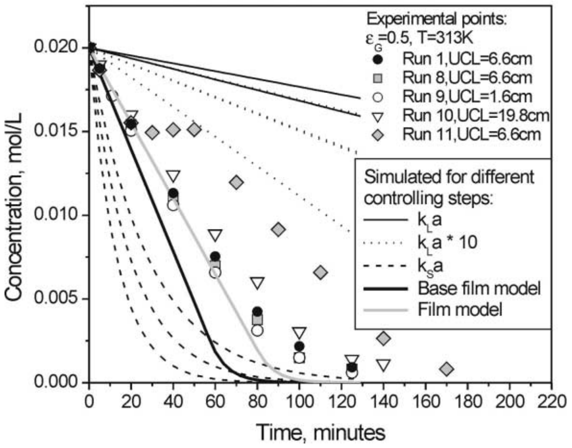

Fig. 3. Influence of the unit cell length on hydrogenation of NBA at 313 K and gas hold-up of 0.5.

where just one reaction step controls the reaction rate. The maximum reaction rates during heterogeneous catalytic reactions are determined by the mass transport. The solution of reactor model for the case where the mass transport is rate-limiting step sets the physical boundaries for the observed process. The discrepancy between the measurements and the predicted boundaries shows that the model is wrong or incomplete. Former facts were taken into account during selection of experimental conditions. To verify the mass transport, we used a wide concentration range. The catalyst utilization was examined by changing the catalyst loading by performing experiments at different gas hold-ups. Impact of mass transport and reaction kinetics on the observed reaction rate was estimated from the results measured at different temperatures. The following comparison will illustrate the wide concentration range used in this investigation. While at high concentrations of NBA, the concentration of hydrogen in saturated solution was about 100 times lower than that required according to stoichiometry for complete reaction, at low concentration of NBA this ratio was around 3. A comparison between model predictions and experimentally measured reaction rate for these two extreme conditions was used to verify equations used for model description.

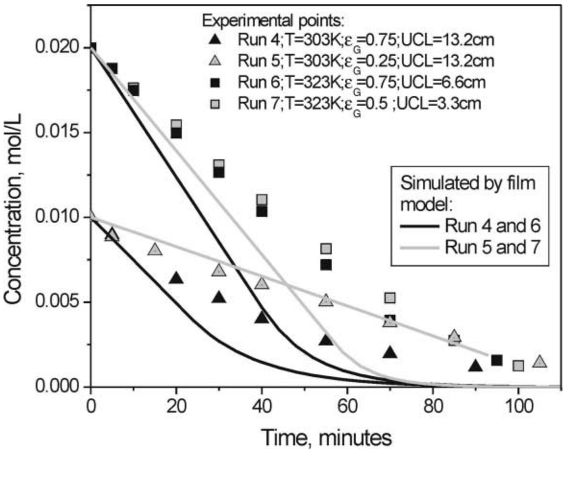

Fig. 4. Comparison between measured and simulated concentration profiles during hydrogenation of NBA at 303 and 323 K and various gas hold-ups.

As it was already mentioned, the model was used for parametric study of hydrogenation of NBA in the one channel monolith reactor. The model was first solved for two hypothetical cases: (A) the overall reaction is controlled by hydrogen mass transport; (B) the overall reaction is controlled by NBA mass transport, and after confrontation with experimental measurement the model was tested also with additional controlling step (C), which assumes that the $k_\mathrm{L}a$ coefficient is 10 times higher than the predicted one by Eq. (3) in order to cover eventual equation uncertainty. To solve the model according to the hypothetical case A, the equations describing hydrogen and NBA consumption were written as:

$$\frac{\mathrm{d}C_{\mathrm{H}_2}}{\mathrm{d}t} = (k_\mathrm{L}a)_{\mathrm{H}_2}(C_{\mathrm{H}_2}^{\mathrm{sat}} - C_{\mathrm{H}_2}) - (k_\mathrm{S}a)_{\mathrm{H}_2}C_{\mathrm{H}_2},$$

$$\frac{\mathrm{d}C_{\mathrm{NBA}}}{\mathrm{d}t} = -(k_\mathrm{S}a)_{\mathrm{H}_2}\frac{C_{\mathrm{H}_2}}{3}. \qquad (8)$$

It was assumed that the reaction rate is much higher than the mass transport and therefore the surface concentration of hydrogen is almost 0. The maximal consumption of NBA is — according to reaction stoichiometry — equal to one-third of hydrogen flux to the surface. The model equation according to the restriction B was written as follows:

$$\frac{\mathrm{d}C_{\mathrm{NBA}}}{\mathrm{d}t} = -(k_\mathrm{S}a)_{\mathrm{NBA}}C_{\mathrm{NBA}}, \qquad (9)$$

since the total consumption of NBA at the catalyst surface was assumed. Equations describing the controlling step C are the same as those under case A. From the analysis presented in Figs. 1 and 2, we can see that the experimental results lie in the area bounded by solutions of the model for cases A–C. It is evident that liquid–solid mass transport of NBA is not the rate limiting step at high concentrations of NBA, while at low concentration range the reaction rate is controlled by NBA mass transport. According to the model prediction, hydrogen mass transport is insufficient for such high conversions. It is obvious that equations for prediction of $k_{\mathrm{L}}a$ and $k_{\mathrm{S}}a$ coefficients, which were derived under non-reacting conditions do not take into account the mass transport of the gaseous reactant (hydrogen) from liquid film to catalyst surface. To estimate the maximal possible impact of that mass transport, a new model based on a film theory was formulated. Based on the UC concept, the mass balance equation for NBA now reads

$$\frac{\mathrm{d}C_{\mathrm{NBA}}}{\mathrm{d}t}V(1-\varepsilon_{\mathrm{G}}) = -\frac{D_{\mathrm{H}_2}A\varepsilon_{\mathrm{G}}(C_{\mathrm{H}_2}^{\mathrm{sat}} - C_{\mathrm{H}_2}^{\mathrm{Surf}})}{3\delta}. \tag{10}$$

If former equations is rearranged and volume V and surface A are expressed by terms defining UC and if we assume complete consumption of hydrogen at the catalyst surface, Eq. (10) transforms to

$$\frac{\mathrm{d}C_{\mathrm{NBA}}}{\mathrm{d}t} = -\frac{4D_{\mathrm{H}_2}\varepsilon_{\mathrm{G}}C_{\mathrm{H}_2}^{\mathrm{sat}}}{3\delta d_T(1-\varepsilon_{\mathrm{G}})}. \tag{11}$$

The reaction course predicted with this equation is shown in Fig. 3 as a curve labeled the base film model. We can see that the prediction is close to the measured concentrations and it is certainly within uncertainties of parameters appearing in the equation. We should bear in mind that diffusion coefficient and hydrogen saturation concentration were calculated from the correlations for pure water and that the film thickness δ was calculated using the correlation obtained in smooth glass tubes. Therefore, we adjusted the equation to meet experiments by decreasing the hydrogen flux for empirical factor of 1.35. In the figures, the predictions obtained by this correction are labeled as film model.

From the results presented in Figs. 1 and 2, it is evident that a good agreement was obtained in the range of high NBA concentrations where it is obvious that the hydrogen mass transport is the rate-limiting step. At low NBA concentrations, reaction is controlled by mass transport of NBA and the process could be well described by model B. From the results presented in Fig. 3, it is clear that at high NBA concentrations the length of UC has negligible influence on the reaction course. This could be explained by a very high NBA/H_2 ratio, which assures that the concentration of NBA in the liquid film nearby the catalyst does not change considerably between two successive liquid slugs and therefore the chemical reaction proceeds almost under the same conditions regardless the length of UC. The results of the runs 1, 8 and 11 show that the experiments were reproducible (no deactivation) and that only physically adsorbed hydrogen entered into the reaction, since no conversion was observed when hydrogen was replaced by nitrogen (from 22 to 51 min).

In the last figure, the influence of temperature and gas hold-up is presented. From the discrepancy between the measured and predicted concentration profiles measured at different temperatures and concentrations it is evident that overall reaction proceeded in the mixed regime. However, the predicted trend is in agreement with the experimental observations. The role of gas hold-up is also connected with concentrations of NBA and hydrogen. While at high NBA concentrations, the overall reaction rate decreased if gas hold-up was decreased (Fig. 4), at lower NBA concentrations (Fig. 2) the overall reaction rate increased if gas hold-up was decreased. From this observation, it can be concluded that the dissolved hydrogen is almost completely consumed in the liquid film, when reactor operates at high NBA concentrations. The similar conclusion can be drawn from the work of Hatziantoniou et al. [6], who studied the hydrogenation of nitrobenzene and *m*-nitrotoluene. At low NBA concentrations, the dissolved hydrogen is not consumed in the liquid film and therefore reaction takes place also when the liquid slug passes the catalyst surface. From the results presented, it is obvious that the catalyst utilization is related to the hydrogen consumption.

Based on the results of this study and considering the previous findings during mass transport studies, a qualitative explanation of the mass transport under non-reactive conditions could be given. During Taylor flow, the liquid and gas pass the capillary in well-defined pattern. The thin liquid film surrounding the tube wall is saturated by the gas (during $k_{\mathrm{L}}a$ measurements) when the gas bubble covers it. In the case of $k_{\mathrm{S}}a$ measurement, the liquid film is saturated with the slightly soluble component nearby the tube wall, which was previously made from that component. When the liquid slug passes the tube it exchanges a part of the liquid with that from the liquid film surrounding the tube wall. Results of RTD measurements [11] showed that approximately 70% of liquid from liquid film bypasses the liquid slug. During mass transport studies, the concentration of soluble components increases along the film towards the next liquid slug which in turn decreases the driving force. Under reaction conditions the driving force is much higher due to the catalytic reaction at the catalyst surface, which keeps the driving force high.

The accuracy of our results could be verified by comparison with the results of Hatziantoniou and Andersson [21], who studied the same reaction in commercial monolith. Despite different experimental set-up and operating conditions the values of determined reaction rates are comparable. This fact confirms our hypothesis that the reaction is appreciably controlled by hydrogen mass transport.

5. Conclusions

The presented results show that the three-phase reactions in the monolith reactors are considerably limited by the mass transport. Models based on empirical correlation for prediction of volumetric mass transport coefficients work well only when solute concentration is low. In the case of low soluble gasses and high concentrated solutions the overall reaction rate in the monolith reactor could be estimated by simple film model. For more accurate predictions the film model should be coupled with reaction kinetics. For the design of monolith reactors by film model the correct determination of film thickness is of a crucial meaning and can be more important than the reaction kinetics, especially when very active catalyst is used.

Acknowledgements

The author gratefully acknowledges the financial support from Slovenian Ministry of Science and Technology under grant No. 104-0521.

References

[1] A. Cybulski, J.A. Moulijn, Structured Catalysts and Reactors, Marcel Dekker, New York, 1998.

[2] A.A. Klinghoffer, R.L. Cerro, M.A. Abraham, Catal. Today 40 (1998) 59–71.

[3] L.L. Crynes, R.I. Cerro, M.A. Abraham, AIChE J. 41 (1995) 337–345.

[4] J. Wärnå, I. Turunen, T. Salmi, T. Maunula, Chem. Eng. Sci. 49 (1994) 5763–5773.

[5] R.K. Edvinsson, A.M. Holmgren, S. Irandoust, Ind. Eng. Chem. Res. 34 (1995) 94–100.

[6] V. Hatziantoniou, B. Andersson, N.H. Schöön, Ind. Eng. Process Des. Dev. 25 (1986) 964–970.

[7] S. Irandoust, B. Andersson, E. Bengtsson, M. Siverström, Ind. Eng. Chem. Res. 28 (1989) 1489–1493.

[8] R.K. Edvinsson, J.A. Moulijn, in: Proceedings of the First European Congress on Chemical Engineering, Florence, Italy, May 4–7, 1997, pp. 1913–1916.

[9] S. Irandoust, S. Ertle, B. Andersson, Can. J. Chem. Eng. 70 (1992) 115–119.

[10] V. Hatziantoniou, B. Andersson, Ind. Eng. Chem. Fund. 21 (1982) 451–456.

[11] G. Berčič, A. Pintar, Chem. Eng. Sci. 52 (21–22) (1997) 3709–3719.

[12] G. Berčič, A. Pintar, J. Batista, in: Proceedings of the First European Congress on Chemical Engineering, Florence, Italy, May 4–7, 1997, pp. 655–658.

[13] D. Alibegić, B.Sc. Thesis, University of Ljubljana, 1997, p. 58.

[14] S. Irandoust, B. Andersson, Ind. Eng. Chem. Res. 28 (1989) 1684–1688.

[15] T.K. Sherwood, R.L. Pigford, C.R. Wilke, Mass Transfer, McGraw-Hill, New York, 1975, pp. 70–80.

[16] C.L. Yaws, Physical Properties, Chemical Engineering, McGraw-Hill, New York, 1977.

[17] R.C. Reid, The Properties of Gases and Liquids, 4th Edition, McGraw-Hill, New York, 1987, p. 598.

[18] R.H. Perry, D. Green, Perry's Chemical Engineering Handbook, 6th Edition, McGraw-Hill, New York, 1984, pp. 3–259.

[19] P.G.T. Fogg, W. Gerrard, Solubility of Gases in Liquids, Wiley, New York, 1991, p. 301.

[20] W.H. Press, S.A. Teukolsky, W.T. Vettering, B.P. Flannery, Numerical Recipes in Fortran, 2nd Edition, Cambridge University Press, Cambridge, 1992, p. 713.

[21] V. Hatziantoniou, B. Andersson, Ind. Eng. Chem. Fund. 23 (1984) 82–88.